surements were performed under argon, at 20 °C. The complexes 1 and 2 were synthesized according to a procedure, which is to be published.[10]

$E°$ values were taken where possible as the average of the anodic and cathodic peak potentials. Electrochemical reversibility was judged on the basis of the peak-to-peak separation (ΔE_p) for the complementary anodic and cathodic cyclovoltammetric waves, relative to the predicted value of 59 mV for a reversible one-electron process.[21,26] IR drop due to solution resistance was not compensated and led to ΔE_p values somewhat greater than the predicted 59 mV.

Acknowledgment. Thanks are due to the Fonds zur Förderung der Wissenschaft und Forschung, Vienna, Austria, for making available the electrochemical equipment.

Diphosphine-Bridged, Heterobimetallic Complexes Containing Iridium and Osmium. Reversible Ortho Metalation of a Bridging Bis(diphenylphosphino)methane Group at the Iridium Center Promoted by the Adjacent Osmium Center

Robert W. Hilts, Roberta A. Franchuk, and Martin Cowie*

Department of Chemistry, The University of Alberta, Edmonton, Alberta, Canada T6G 2G2

Received August 8, 1990

The compound (PPN)[$HOs(CO)_4$] reacts readily with [$IrCl(\eta^2$-dppm$)_2$] ($PPN^+ = (Ph_3P)_2N^+$, dppm = $Ph_2PCH_2PPh_2$) at ambient temperature, yielding the heterobinuclear complex [$IrOs(H)_2(CO)_3(\mu_2$-η^3-(o-C_6H_4)$PhPCH_2PPh_2$)(dppm)] (1), in which one phenyl group is ortho-metalated at the Ir center. Treatment of 1 with the electrophile sources HBF_4·Et_2O or [$AuPPh_3$]BF_4 reverses the ortho metalation to give the hydrido-bridged species, [$IrOs(CO)_3(\mu$-H)(μ-X)(dppm)$_2$][BF_4] (X = H (2), $AuPPh_3$ (3)). Deprotonation of 2 with use of NaH regenerates compound 1. The $AuPPh_3$ group in 3 is readily replaced by an iodo group in the reaction with I_2 to give [$IrOs(CO)_3(\mu$-H)(μ-I)(dppm)$_2$][BF_4] (4). Under a CO atmosphere, compound 2 yields [$IrOs(CO)_5$(dppm)$_2$][BF_4] (5), and reaction of 5 with Me_3NO·$2H_2O$ results in loss of one carbonyl group from the Ir center to yield [$IrOs(CO)_4$(dppm)$_2$][BF_4] (6). The structure of 5 has been determined by X-ray techniques. This compound crystallizes, together with 1.5 equiv of CH_2Cl_2, in the monoclinic space group $P2_1/c$, with cell parameters a = 12.063 (2) Å, b = 22.725 (3) Å, c = 22.050 (3) Å, β = 101.66 (1)°, V = 5920 Å^3, and Z = 4. The structure has refined to R = 0.043 and R_W = 0.063 on the basis of 5515 unique observations with 444 parameters varied. Compound 5 has a trans-bridging arrangement of diphosphine ligands and has two carbonyls bound to Ir and three on Os. The carbonyl and phosphine arrangement on Os suggests a trigonal bipyramidal (TBP) arrangement characteristic of Os(0), which then forms a dative Os → Ir bond to the Ir(+I) center, giving it a TBP geometry also. The Os–Ir separation of 2.9652 (4) Å is at the long end of the range expected for a normal single bond.

Introduction

Our ongoing interests in metal–metal cooperativity effects in binuclear complexes[1] have recently expanded to include complexes containing two different metals.[2-8] Most of the heterobinuclear complexes studied by us to date contain Rh as one of the metals and have been derived from the precursors, [(OC)Rh(μ-dppm)$_2$$MH_x(CO)_y$] (M = Co, Ir, x = 0, y = 2; M = Fe, Ru, Os, x = 1, y = 2; M = Mn, Re, x = 0, y = 3; M = Cr, W, x = 1, y = 3; dppm = $Ph_2PCH_2PPh_2$).[4] These compounds have been formulated as containing a Rh(+I) center with an accompanying M → Rh donor–acceptor bond,[4,8] as shown in the drawing below, and join the growing list of compounds for which a metal–metal dative bond appears to be present.[9] Such

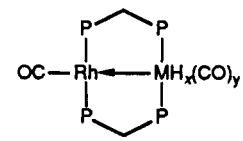

bonds have been shown to be relatively labile,[9b] so they may be a source of incipient coordinative unsaturation in these diphosphine-bridged complexes. We are interested in obtaining additional information about the natures of these metal–metal interactions, about the subtle electron redistributions that might occur during reactions, and about the effect of the dative M → Rh bond on the re-

(1) See for example: (a) Sutherland, B. R.; Cowie, M. *Organometallics* **1985**, *4*, 1637. (b) Sutherland, B. R.; Cowie, M. *Organometallics* **1985**, *4*, 1801. (c) Cowie, M.; Vasapollo, G.; Sutherland, B. R.; Ennett, J. P. *Inorg. Chem.* **1986**, *25*, 2648. (d) Vaartstra, B. A.; Cowie, M. *Organometallics* **1990**, *9*, 1594.
(2) Vaartstra, B. A.; Cowie, M. *Inorg. Chem.* **1989**, *28*, 3138.
(3) Vaartstra, B. A.; Cowie, M. *Organometallics* **1989**, *8*, 2380.
(4) Antonelli, D. M.; Cowie, M. *Organometallics* **1990**, *9*, 1818.
(5) Antonelli, D. M.; Cowie, M. *Inorg. Chem.* **1990**, *29*, 3339.
(6) Antonelli, D. M.; Cowie, M. *Inorg. Chem.* **1990**, *29*, 4039.
(7) Hilts, R. W.; Franchuk, R. A.; Cowie, M. *Organometallics* **1991**, *10*, 304.
(8) McDonald, R.; Cowie, M. *Inorg. Chem.* **1990**, *29*, 1564.
(9) (a) Roberts, D. A.; Mercer, W. C.; Zahurak, S. M.; Geoffroy, G. L.; De Brosse, C. W.; Cass, M. E.; Pierpont, C. G. *J. Am. Chem. Soc.* **1982**, *104*, 910. (b) Roberts, D. A.; Mercer, W. C.; Geoffroy, G. L.; Pierpont, C. G. *Inorg. Chem.* **1986**, *25*, 1439. (c) Meyer, T. J. *Prog. Inorg. Chem.* **1975**, *19*, 1. (d) Hames, B. W.; Legzdins, P. *Organometallics* **1982**, *1*, 116. (e) Barr, R. D.; Marder, T. B.; Orpen. A. G.; Williams, I. D. *J. Chem. Soc., Chem. Commun.* **1984**, 112. (f) Einstein, F. W. B.; Pomeroy, R. K.; Rushman, P.; Willis, A. C. *J. Chem. Soc., Chem. Commun.* **1983**, 854. (g) Einstein, F. W. B.; Jones, T.; Pomeroy, R. K.; Rushman, P. *J. Am. Chem. Soc.* **1984**, *106*, 2707. (h) Einstein, F. W. B.; Pomeroy, R. K.; Rushman, P.; Willis, A. C. *Organometallics* **1985**, *4*, 250. (i) Davis, H. B.; Einstein, F. W. B.; Glavina, P. G.; Jones, T.; Pomeroy, R. K.; Rushman, P. *Organometallics* **1989**, *8*, 1030. (j) Batchelor, R. J.; Davis, H. B.; Einstein, F. W. B.; Pomeroy, R. K. *J. Am. Chem. Soc.* **1990**, *112*, 2036. (k) Cowie, M.; Dickson, R. S. *J. Organomet. Chem.* **1987**, *326*, 269.

0276-7333/91/2310-1297$02.50/0

activity of the coordinatively unsaturated Rh center. Since much of our interest in these low-valent complexes concerns their binuclear oxidative-addition reactions, it was an obvious extension of our previous work involving Rh to investigate analogous complexes of Ir. Assuming a square-planar Ir(I) formulation, analogous to that found for several of the Rh species[4,8,10] and as diagramed above, the Ir centers in these complexes would clearly be related to that in Vaska's compound, $[IrCl(CO)(PPh_3)_2]$, known to have a rich chemistry involving oxidative-addition reactions. In this paper, we present the first of our studies on diphosphine-bridged, heterobinuclear complexes of iridium and osmium.

Experimental Section

All solvents were dried and distilled over the appropriate dessicants immediately before their use. Reactions were performed at room temperature by using standard Schlenk techniques. Prepurified argon gas was used directly from the cylinder without additional drying. Hydrated iridium(III) chloride was obtained from Engelhard Scientific Ltd., while bis(diphenylphosphino)methane (dppm), tetrafluoroboric acid-diethyl ether ($HBF_4 \cdot Et_2O$), methyl triflate ($CH_3SO_3CF_3$), sodium hydride (60% dispersion in oil), triphenylphosphinegold(I) chloride ($Au(PPh_3)Cl$), hydrated trimethylamine oxide ($Me_3NO \cdot 2H_2O$), silver tetrafluoroborate ($AgBF_4$), iodine (I_2), trimethylphosphine (PMe_3), dimethyl acetylenedicarboxylate (DMAD), and triosmium dodecacarbonyl ($Os_3(CO)_{12}$) were purchased from Aldrich. The hexafluoro-2-butyne (HFB) was obtained from SCM Specialty Chemicals and the carbon-13-labeled carbon monoxide (99% enriched) was purchased from Isotec, Inc. The compounds $[Ir(C_8H_{14})_2(\mu\text{-}Cl)]_2$[11] and $(PPN)[HOs(CO)_4]$[12] were prepared by the reported procedures.

The $^{31}P\{^1H\}$ and $^{31}P\{^{31}P\}$ NMR spectra were recorded on a Bruker AM-400 Fourier transform spectrometer operating at 161.98 MHz. ^1H and $^1H\{^{31}P\}$ spectra were also obtained on this instrument at 400.1 MHz. Proton-decoupled carbon-13 NMR spectra were run on either a Bruker AM-300 spectrometer at 75.5 MHz or the AM-400 instrument at 100.6 MHz. The $^{13}C\{^1H\}$ NMR experiments with selective ^{31}P decoupling were performed on a Bruker AM-200 spectrometer at 50.32 MHz. Phosphorus-31 chemical shifts are referenced to 85% H_3PO_4, while carbon-13 and proton shifts are with respect to TMS. In all cases, the NMR spectrometer was locked to the solvent deuterium resonance. Infrared spectra were run on a Nicolet 7199 Fourier transform interferometer, either as Nujol mulls or as dichloromethane casts on KBr plates. Elemental analyses were performed by the analytical service within the department. The $^{31}P\{^1H\}$ NMR spectrum for compound 1 was simulated by using the PANIC program supplied by Bruker.

Preparation of the Compounds. Selected spectroscopic data for compounds 1-6 are provided in Table I.

(a) $[IrCl(\eta^2\text{-dppm})_2]$. All glassware was dried at 100 °C for 24 h and then assembled while hot. A three-necked, round-bottomed flask, equipped with two gas outlets and a septum, was charged with $[Ir(C_8H_{14})_2(\mu\text{-}Cl)]_2$ (0.100 g, 0.112 mmol) and dppm (0.172 g, 0.448 mmol). Benzene (15 mL) was added by cannula directly from the distillation vessel, and the resulting yellow solution was stirred under argon for 1 h. At the end of this time, the benzene was removed in vacuo, leaving a pale-yellow powder that was kept under vacuum for an additional hour. Dissolution of the yellow residue in 3 mL of CH_2Cl_2, followed by cooling of the resulting solution to -18 °C, afforded $[IrCl(\eta^2\text{-dppm})_2]$ (0.189 g, 0.190 mmol) as a yellow crystalline solid. Yield: 85%. Anal. Calcd for $C_{50}H_{44}ClIrP_4$: C, 60.27; H, 4.45; Cl, 3.56. Found: C, 60.07; H, 4.72; Cl, 4.18. $^{31}P\{^1H\}$ NMR spectrum (CD_2Cl_2, 22 °C): δ -55.15 (singlet).

(b) $[IrOs(H)_2(CO)_3(\mu_2\text{-}\eta^3\text{-}(o\text{-}C_6H_4)PhPCH_2PPh_2)(dppm)]$ (1). A pale-yellow solution of $(PPN)[HOs(CO)_4]$ (0.188 g, 0.223 mmol) in 20 mL of THF was added by cannula to a stirred, yellow solution of $[IrCl(\eta^2\text{-dppm})_2]$ (0.222 g, 0.223 mmol) in 25 mL of THF. The mixture was stirred under a stream of argon at room temperature for 16 h. A fine, colorless precipitate began to form after the first hour of stirring, and the solution gradually became a paler shade of yellow. By the end of the reaction period, the solvent volume had been reduced to approximately 20 mL. Diethyl ether (20 mL) was added to effect complete precipitation of the (PPN)Cl byproduct. The precipitate was allowed to settle, the clear supernatant was transferred by syringe to another flask, and the solvent was removed under vacuum. Recrystallization of the yellow residue from THF/hexane afforded frondlike, yellow crystals of compound 1 (0.207 g, 0.167 mmol). Yield: 75%. Anal. Calcd for $C_{53}H_{45}IrO_3OsP_4$: C, 51.49; H, 3.67. Found: C, 51.77; H, 3.88.

(c) $[IrOs(CO)_3(\mu\text{-}H)_2(dppm)_2][BF_4]$ (2). A solution of $HBF_4 \cdot Et_2O$ (0.014 g, 0.084 mmol) in 20 mL of Et_2O was added via cannula to a stirred slurry of 1 (0.100 g, 0.081 mmol) in a mixture of 1 mL of THF and 10 mL of Et_2O. An immediate color change from dark to pale yellow was observed, and a fluffy yellow precipitate formed. The solution was stirred for 1 h, the colorless supernatant was discarded, and the remaining yellow solid was washed with hexane (2 × 20 mL) and kept under vacuum for 3 h. Extraction of the yellow residue with 3 mL of CH_2Cl_2, followed by the slow addition of 10 mL of Et_2O resulted in the formation of small yellow crystals of $[IrOs(CO)_3(\mu\text{-}H)_2(dppm)_2][BF_4]$ (0.081 g, 0.061 mmol). Yield: 75%. Anal. Calcd for $C_{53}H_{46}BF_4IrO_3OsP_4$: C, 48.08; H, 3.50. Found: C, 48.33; H, 3.27.

(d) $[IrOs(CO)_3(\mu\text{-}H)(\mu\text{-}AuPPh_3)(dppm)_2][BF_4]$ (3). A solution of $[Au(PPh_3)Cl]$ (0.076 g, 0.154 mmol) in 15 mL of freshly distilled acetone was added by syringe to a flask containing crystalline $AgBF_4$ (0.030 g, 0.155 mmol), causing the immediate precipitation of a colorless solid. After 1 h of stirring, the purple-gray mixture was filtered to remove precipitated AgCl, and the solvent was removed under vacuum. The colorless residue was dissolved in 15 mL of THF, and the resulting solution was added via cannula to a stirred yellow solution of compound 1 (0.190 g, 0.154 mmol) in 20 mL of THF, causing the immediate formation of a red-brown solution. After 1 h of stirring, the reaction mixture was filtered and the solvent was removed under vacuum. Recrystallization of the remaining brick-red solid from CH_2Cl_2/Et_2O at room temperature afforded $[IrOs(CO)_3(\mu\text{-}H)(\mu\text{-}AuPPh_3)(dppm)_2][BF_4]$ (0.216 g, 0.121 mmol) as orange-red crystals. Yield: 79%. Anal. Calcd for $C_{71}H_{60}AuBF_4IrO_3OsP_5$: C, 47.85; H, 3.39. Found: C, 47.77; H, 3.30.

(e) $[IrOs(CO)_3(\mu\text{-}H)(\mu\text{-}I)(dppm)_2][BF_4]$ (4). A solution of I_2 (0.014 g, 0.056 mmol) in 20 mL of CH_2Cl_2 was added dropwise over a period of 1 h to a stirred solution of $[IrOs(CO)_3(\mu\text{-}H)(\mu\text{-}AuPPh_3)(dppm)_2][BF_4]$ (0.200 g, 0.112 mmol) in 20 mL of CH_2Cl_2, resulting in a gradual change in color from red-brown to yellow. The mixture was stirred for an additional hour, and the solvent was removed under vacuum. The resulting yellow residue was washed with 2 × 20 mL of Et_2O and recrystallized from THF/Et_2O to give $[IrOs(CO)_3(\mu\text{-}H)(\mu\text{-}I)(dppm)_2][BF_4] \cdot THF$ (0.137 g, 0.090 mmol) as a dull-yellow solid. Yield: 80%. The side product $[Au(PPh_3)I]$ was detected in the reaction mixture ($^{31}P\{^1H\}$: δ 39.08 in CD_2Cl_2) but was not isolated. The presence of 1 M equiv of THF was confirmed by ^1H and ^{13}C NMR spectroscopy. Anal. Calcd for $C_{57}H_{53}BF_4IrO_4OsP_4$: C, 44.98; H, 3.51; I, 8.34. Found: C, 45.19; H, 3.44; I, 7.67.

(f) $[IrOs(CO)_5(dppm)_2][BF_4]$ (5). A solution of $[IrOs(CO)_3(\mu\text{-}H)_2(dppm)_2][BF_4]$ (2) (0.100 g, 0.076 mmol) in 20 mL of CH_2Cl_2 was stirred under a stream of CO gas for 36 h. The solvent volume was kept at approximately 20 mL through the periodic addition of freshly distilled CH_2Cl_2. At the end of the reaction period, the solvent was removed under vacuum, and the residue was washed with 10 mL of THF followed by 2 × 20 mL of Et_2O. Recrystallization from CH_2Cl_2/Et_2O afforded yellow crystals of $[IrOs(CO)_5(dppm)_2][BF_4]$ (0.101 g, 0.073 mmol). Yield: 96%. Anal. Calcd for $C_{55}H_{44}BF_4IrO_5OsP_4$: C, 47.94; H, 3.22. Found: C, 47.74; H, 3.52.

(g) $[IrOs(CO)_4(dppm)_2][BF_4]$ (6). A solution of $Me_3NO \cdot 2H_2O$ (0.012 g, 0.109 mmol) in 20 mL of CH_3CN was added dropwise over a period of 1 h with a continuous argon purge to a stirred

(10) (a) Elliot, D. J.; Ferguson, G.; Holah, D. G.; Hughes, A. N.; Jennings, M. C.; Magnuson, V. R.; Potter, D.; Puddephatt, R. J. *Organometallics* **1990**, *9*, 1336. (b) Puddephatt, R. J. Personal communication.

(11) Herde, J. L.; Lambert, J. C.; Senoff, C. F. *Inorg. Synth.* **1974**, *15*, 19.

(12) Walker, H. W.; Ford, P. C. *J. Organomet. Chem.* **1981**, *214*, C43.

Table I. Selected Spectroscopic Data for the Compounds[a]

compd	IR, cm^{-1} [b]	NMR[c] δ ($^{31}P\{^1H\}$)	NMR[c] δ ($^{13}C\{^1H\}$)	NMR[c] δ (^1H)
1	1910 (ss), 1915 (ss), 1920 (ss), 1974 (ss), 2018 (ws)[d]	P_A −6.49 (ddd), P_B −17.08 (ddd), P_C −20.32 (ddd),[e,f] P_D −22.91 (ddd), $J(P_AP_B)$ = 390 Hz, $J(P_AP_C)$ = 92 Hz, $J(P_AP_D)$ = 16 Hz, $J(P_BP_C)$ = 24 Hz, $J(P_BP_D)$ = 54 Hz, $J(P_CP_D)$ = 17 Hz	OsCO (CO(1), 189.84 (d, 1 C, ^2J(PC) = 88 Hz); (CO(2), 168.89 (s, 1 C); IrCO (CO(3), 180.92 (d, 1 C, $^2J(H_{(2)}C)$ = 27 Hz)	H_A 3.46 (ddd, 1 H); H_B 5.55 (ddd, 1 H, $^2J(H_AH_B) = {}^2J(P_CH_B) = {}^2J(P_AH_A) = {}^2J(P_CH_A) = {}^2J(P_AH_B)$ = 14 Hz); H_C 3.70 (ddd, 1 H); H_D 4.92 (dddd, 1 H, $^2J(H_CH_D) = {}^2J(P_BH_C)$ = 14 Hz, $^2J(P_DH_C)$ = 6 Hz, $^4J(P_AH_C)$ = 2 Hz, $J(P_BH_D)$ = 6 or 14 Hz, $^2J(P_DH_D)$ = 6 or 14 Hz, $^4J(H_{(1)}H_D)$ = 7 Hz); OsH($H_{(1)}$) −9.50 (dddd, 1 H, $^2J(P_CH_{(1)})$ = 65 Hz, $^3J(P_AH_{(1)})$ = 7 Hz, $^2J(P_DH_{(1)})$ = 27 Hz, $^4J(H_{(1)}H_D)$ = 7 Hz); IrH($H_{(2)}$) −12.60 (ddd, 1 H, $^2J(P_AH_{(2)}) = {}^2J(P_BH_{(2)})$ = 14 Hz, $^3J(P_DH_{(2)})$ = 18 Hz)
2[h]	1958 (sb), 1975 (sh), 2038 (ms)	14.11 (IrP), 0.52 (OsP), N[g] = 109 Hz	OsCO 180.62 (t, 2 C, ^2J(PC) = 7 Hz);[h] IrCO 177.83 (t, 1 C, ^2J(PC) = 15 Hz)	PCH_2P 4.26 (m, 4 H); OsHIr −9.42 (tt, 2 H, ^2J(IrP-H) = ^2J(OsP-H) = 14 Hz)
3[h]	1940 (sb), 1999 (ms)	13.27 (IrP), −1.47 (OsP), N = 112 Hz, 51.22 (OsAu$P$$Ph_3$Ir, t, ^3J(OsP-AuP) = 10 Hz)	OsCO 183.69 (dt, 1 C, ^2J(OsP-C) = 10 Hz, ^3J(AuP-C) = 13 Hz), 188.10 (dt, 1 C, ^2J(OsP-C) = 7 Hz, ^3J(AuP-C) = 3 Hz); IrCO 179.05 (dt, 1 C, ^2J(IrP-C) = 15 Hz, ^3J(AuP-C) = 4 Hz)	PCH_2P (AB) 3.98 (m, 2 H), 5.40 (m, 2 H, ^2J(HH) = 12 Hz); OsHIr −9.72 (dtt, 1 H, ^3J(AuP-H) = 4 Hz, ^2J(IrP-H) = 7 Hz, ^2J(OsP-H) = 11 Hz)
4[h]	1952 (ss), 1984 (ss), 2034 (ss), 2049 (sh)	−3.52 (IrP), −18.21 (OsP), N = 71 Hz	OsCO 174.91 (t, 1 C, ^2J(PC) = 9 Hz); OsCO/IrCO 172.79 (t, 1 C, ^2J(PC) = 9 Hz), 166.89 (t, 1 C, ^2J(PC) = 10 Hz)	PCH_2P (AB) 4.42 (dm, 2 H), 4.69 (dm, 2 H, ^2J(HH) = 14 Hz); OsHIr −13.08 (tt, 1 H, ^2J(OsP-H) = ^2J(IrP-H) = 9 Hz)
5[h]	1903 (ms), 1942 (ss), 1949 (ss), 1979 (ss), 2018 (ms)	−15.23 (OsP), −9.46 (IrP), N = 76 Hz	OsCO 174.13 (t, 1 C, ^2J(PC) = 10 Hz), 199.53 (t, 2 C, ^2J(PC) = 10 Hz); IrCO 184.48 (t, 2 C, ^2J(PC) = 13 Hz)	PCH_2P 4.57 (m, 4 H)
6[h]	1930 (sh), 1959 (ss), 2020 (ws)[i]	18.26 (IrP), −8.43 (OsP), N = 108 Hz	OsCO 192.62 (t, 2 C, ^2J(PC) = 9 Hz),[j] 182.30 (t, 1 C, ^2J(PC) = 11 Hz); IrCO 175.30 (t, 1 C, ^2J(PC) = 12 Hz)	PCH_2P 4.49 (m, 4 H)

[a] Abbreviations used: For IR, (ss) strong sharp, (sb) strong broad, (ms) medium sharp, (ws) weak sharp, (sh) shoulder. For NMR, (s) singlet, (d) doublet, (t) triplet, (dt) doublet of triplets, (dtt) doublet of triplets of triplets, (tt) triplet of triplets, (dm) doublet of multiplets, (m) multiplet, (ddd) doublet of doublets of doublets, (dddd) doublet of doublets of doublets of doublets. [b] Unless otherwise noted, bands listed are carbonyl stretches and spectra were recorded in Nujol. [c] Spectra were recorded in CD_2Cl_2 unless otherwise noted. [d] ν(M-H). [e] Labeling scheme is shown in the text. [f] NMR spectra were recorded in d^8-THF. [g] $N = |J(AB) + J(AB')|$. [h] $^{13}C\{^1H\}$ NMR spectrum was recorded at −40 °C. [i] CH_2Cl_2 cast. [j] CD_3CN solution. [k] A broad BF_4^- stretch was observed at ca. 1056 cm^{-1} in the IR spectrum.

solution of $[IrOs(CO)_5(dppm)_2][BF_4]$ (0.150 g, 0.109 mmol) in 20 mL of CH_3CN, resulting in a gradual change in color from yellow to yellow-orange. The mixture was filtered, and the solvent was removed under vacuum, leaving a yellow-orange solid. Recrystallization of the residue from CH_3CN/Et_2O at room temperature afforded $[IrOs(CO)_4(dppm)_2][BF_4]$ (0.103 g, 0.076 mmol) as yellow-orange crystals. Yield: 70%. Anal. Calcd for $C_{54}H_{44}BF_4IrO_4OsP_4$: C, 48.04; H, 3.29. Found: C, 48.11; H, 3.40.

Reaction of H_2 with Compound 5. A solution of $[IrOs(CO)_5(dppm)_2][BF_4]$ (0.050 g, 0.036 mmol) in 20 mL of CH_2Cl_2 was stirred under a stream of H_2 gas for 36 h. The solvent volume was kept close to 20 mL by periodic additions of fresh CH_2Cl_2. At the end of the reaction period, the solvent was removed under vacuum, leaving a yellow solid that was shown to be essentially pure **2** by $^{31}P\{^1H\}$ NMR and IR spectroscopy.

Reaction of Compound 6 with CO. Bubbling CO gas through a solution of $[IrOs(CO)_4(dppm)_2][BF_4]$ (0.050 g, 0.037 mmol) in 10 mL of CH_2Cl_2 for 1 h resulted in the quantitative formation of $[IrOs(CO)_5(dppm)_2][BF_4]$ (**5**), as shown by $^{31}P\{^1H\}$ NMR and IR spectroscopy.

Reaction of Compound 2 with Sodium Hydride. Tetrahydrofuran (5 mL) was added via syringe to a mixture of sodium hydride (0.050 g, 1.25 mmol, 60% dispersion in oil) and $[IrOs(CO)_3(\mu\text{-}H)_2(dppm)_2][BF_4]$ (0.100 g, 0.076 mmol), and the resulting slurry was stirred vigorously for 1 h. At the end of this time, the unreacted NaH was allowed to settle, and the clear yellow su-

Table II. Crystallographic Data for $[IrOs(CO)_5(dppm)_2][BF_4]\cdot 1.5CH_2Cl_2$ (5)

formula	$C_{55}H_{44}BF_4IrO_5OsP_4\cdot 1.5CH_2Cl_2$
fw	1505.47
space group	$P2_1/c$ (No. 14)
temp, °C	22
radiation (λ, Å)	graphite-monochromated Mo Kα (0.71069)
unit cell parameters	
a, Å	12.063 (2)
b, Å	22.725 (3)
c, Å	22.050 (3)
β, deg	101.66 (1)
V, Å^3	5920 (2)
Z	4
ρ(calcd), g·cm^{-3}	1.683
linear abs coeff (μ), cm^{-1}	46.411
range of transm factors	0.7784–1.4360
R	0.043
R_w	0.063

pernatant was transferred to a second flask. The solvent was then removed under vacuum, leaving a yellow residue that was identified by $^{31}P\{^1H\}$ and ^1H NMR spectroscopy as essentially pure 1. Yield: ≅ 100%.

Attempted Reaction of Compound 5 with Trimethylphosphine and Activated Alkynes. Dichloromethane solutions of 5 were charged with 1 M equiv of either PMe_3 or RC≡CR (R = CO_2Me, CF_3), and the mixtures were stirred for 6 h under a slow argon purge. Phosphorus-31 NMR spectroscopy showed that, in all cases, compound 5 failed to react with the added ligand.

X-ray Data Collection. Yellow crystals of $[IrOs(CO)_5(dppm)_2][BF_4]\cdot 1.5CH_2Cl_2$ (5) were obtained by slow diffusion of Et_2O into a concentrated solution of the complex in CH_2Cl_2. A suitable crystal was mounted on a glass fiber. Preliminary data were collected on an Enraf-Nonius CAD4 diffractometer with use of Mo K_α radiation (λ = 0.71069 Å). Unit cell parameters were obtained by least-squares analyses of 25 carefully centered reflections in the range $22.0 \le 2\theta \le 26.0°$. A monoclinic cell was established by the usual peak search and indexing programs. The systematic absences ($h0l$, l = odd, $0k0$, k = odd), together with the monoclinic diffraction symmetry established the space group as $P2_1/c$.

Intensity data were collected at 22 °C by using the $\theta/2\theta$ scan technique to a maximum of $2\theta = 50.0°$. Backgrounds were scanned for 25% of the peak width on either side of the peak. Three reflections, chosen as intensity standards, were remeasured every 120 min of X-ray exposure time. There was no significant systematic decrease in the intensities of these standards, so no correction was applied. A total of 8539 unique reflections were measured and processed in the usual manner, by using a value for p of 0.04[13] to downweigh intense reflections; of these, 5515 were found to be observed and were used in subsequent calculations. The method of Walker and Stuart[14,15] was used to apply absorption corrections to the data.

Structure Solution and Refinement. The structure was solved in the space group $P2_1/c$ by using standard Patterson, Fourier, and full-matrix, least-squares techniques. Since the Ir and Os atoms could not be distinguished, both metals were input as Os atoms in the initial refinements. These atoms were identified on the basis of their coordination numbers, with Os having one more carbonyl group than Ir, and were given their appropriate scattering factors in subsequent refinements. Atomic scattering factors[16,17] and anomalous dispersion terms[18] were obtained from the usual sources. All of the hydrogen atoms, with the exception of the methylene chloride hydrogens, were included as fixed contributions. Their idealized positions were calculated from the geometries of the attached carbon atom with a C–H distance of 0.95 Å being used. The hydrogen atoms were not refined but were given thermal parameters 20% greater than the isotropic *B*'s of their attached carbon atoms. All non-hydrogen atoms were found, and the final model converged to $R = 0.043$ and $R_w = 0.063$ with 444 parameters varied. The 10 highest residuals (0.5–0.9 e/Å^3) in the final difference Fourier map were located near the BF_4^- counterion and the methylene chloride molecules. Two independent molecules of CH_2Cl_2 were located, both occupying general positions but one having only half-occupancy. The phenyl carbons of dppm, the methylene chloride carbons, and the boron atom of BF_4^- were refined with isotropic thermal parameters. All other non-hydrogen atoms, including the Cl atoms of the CH_2Cl_2 molecules, were refined anisotropically. A summary of the crystal data and the details of intensity measurements are provided in Table II. The fractional atomic coordinates and thermal parameters for the core atoms of compound 5 are collected in Table III, while selected bond lengths and angles for this structure can be found in Tables IV and V, respectively. Additional information is presented as supplementary material.

Table III. Positional and Thermal Parameters for Selected Non-Hydrogen Atoms of $[IrOs(CO)_5(dppm)_2][BF_4]\cdot 1.5CH_2Cl_2$ (5)[a]

atom	*x*	*y*	*z*	*B*, Å^2
Ir	0.10500 (3)	0.01674 (2)	0.34317 (2)	2.708 (9)
Os	0.21176 (3)	0.01836 (2)	0.23329 (2)	2.972 (9)
P(1)	0.1796 (2)	0.1089 (1)	0.3762 (1)	2.74 (6)
P(2)	0.2869 (2)	0.1139 (1)	0.2607 (1)	3.08 (6)
P(3)	0.0107 (2)	−0.0710 (1)	0.3108 (1)	2.96 (6)
P(4)	0.1219 (2)	−0.0722 (1)	0.1990 (1)	3.38 (6)
O(1)	−0.1128 (6)	0.0826 (4)	0.2944 (4)	6.3 (2)
O(2)	0.2010 (9)	−0.0358 (4)	0.4679 (4)	7.7 (3)
O(3)	−0.0091 (7)	0.0828 (4)	0.1743 (4)	6.1 (2)
O(4)	0.3498 (8)	0.0081 (4)	0.1316 (4)	8.6 (3)
O(5)	0.3777 (6)	−0.0430 (4)	0.3396 (4)	5.8 (2)
C(1)	−0.0311 (8)	0.0572 (5)	0.3108 (5)	4.0 (3)
C(2)	0.168 (1)	−0.0162 (5)	0.4210 (5)	5.0 (3)
C(3)	0.0718 (9)	0.0579 (5)	0.1963 (5)	4.1 (3)
C(4)	0.297 (1)	0.0123 (5)	0.1697 (6)	5.3 (3)
C(5)	0.310 (1)	−0.0194 (5)	0.3033 (6)	4.5 (3)
C(6)	0.2041 (9)	0.1527 (4)	0.3097 (5)	3.5 (3)
C(7)	−0.0102 (9)	−0.0813 (5)	0.2265 (5)	3.7 (3)

[a] All atoms are refined anisotropically and are given in the form of the isotropic equivalent displacement parameter defined as $^4/_3[a^2\beta(1,1) + b^2\beta(2,2) + c^2\beta(3,3) + ab(\cos\gamma)\beta(1,2) + ac(\cos\beta)\beta(1,3) + bc(\cos\alpha)\beta(2,3)]$.

Table IV. Selected Bond Lengths (Å) for $[IrOs(CO)_5(dppm)_2][BF_4]\cdot 1.5CH_2Cl_2$ (5)[a]

(a) Bonded					
Ir–Os	2.9652 (4)	Os–P(2)	2.383 (2)	O(1)–C(1)	1.136 (9)
Ir–P(1)	2.337 (2)	Os–P(4)	2.378 (2)	O(2)–C(2)	1.13 (1)
Ir–P(3)	2.335 (2)	Os–C(3)	1.941 (9)	O(3)–C(3)	1.148 (9)
Ir–C(1)	1.892 (9)	Os–C(4)	1.91 (1)	O(4)–C(4)	1.16 (1)
Ir–C(2)	1.888 (9)	Os–C(5)	1.95 (1)	O(5)–C(5)	1.15 (1)
(b) Nonbonded					
Ir–C(3)	3.316 (8)	C(1)–C(11)	3.18 (1)	C(4)–H(36)	2.56
Ir–C(5)	2.905 (9)	C(1)–C(3)	3.03 (1)	C(5)–H(26)	2.70
P(1)–P(2)	3.084 (3)	O(5)–H(26)	2.40	C(5)–H(76)	2.52
P(3)–P(4)	3.036 (3)	C(3)–H(36)	2.74		

[a] Numbers in parentheses are estimated standard deviations in the least significant digits.

Results and Discussion

In previous studies, we have demonstrated a convenient route to diphosphine-bridged, heterobinuclear complexes, $[(OC)Rh(\mu\text{-dppm})_2MH_x(CO)_y]$ (M = Co, $x = 0$, $y = 2$; M = Fe, Ru, Os, $x = 1$, $y = 2$; M = Mn, Re, $x = 0$, $y = 3$; M

(13) Doedens, R. J.; Ibers, J. A. *Inorg. Chem.* **1967**, *6*, 204.
(14) Walker, N.; Stuart, D. *Acta Crystallogr., Sect. A: Found Crystallogr.* **1983**, *A39*, 1581.
(15) Programs used were those of the Enraf-Nonius Structure Determination Package by B. A. Frenz, in addition to local programs by R. G. Ball.
(16) Cromer, D. J.; Waber, J. T. *International Tables for X-Ray Crystallography*; Kynoch Press: Birmingham, England, 1974; Vol. IV, Table 2.2A.
(17) Stewart, R. F.; Davidson, E. R.; Simpson, W. T. *J. Chem. Phys.* **1965**, *42*, 3175.
(18) Cromer, D. T.; Liberman, D. *J. Chem. Phys.* **1970**, *53*, 1891.

Table V. Selected Angles (deg) for $[IrOs(CO)_5(dppm)_2][BF_4]\cdot 1.5CH_2Cl_2$ (5)[a]

Os-Ir-P(1)	92.30 (5)	P(2)-Os-C(3)	86.5 (3)	Ir-P(3)-C(51)	111.6 (3)
Os-Ir-P(3)	91.51 (5)	P(2)-Os-C(4)	91.0 (3)	Ir-P(3)-C(61)	121.9 (3)
Os-Ir-C(1)	99.9 (3)	P(2)-Os-C(5)	93.5 (3)	Os-P(4)-C(7)	111.4 (3)
Os-Ir-C(2)	125.8 (3)	P(4)-Os-C(3)	88.0 (3)	Os-P(4)-C(71)	118.5 (3)
P(1)-Ir-P(3)	173.58 (7)	P(4)-Os-C(4)	89.0 (3)	Os-P(4)-C(81)	114.1 (3)
P(1)-Ir-C(1)	86.1 (3)	P(4)-Os-C(5)	92.0 (3)	Ir-C(1)-O(1)	176.4 (8)
P(1)-Ir-C(2)	90.7 (3)	C(3)-Os-C(4)	106.2 (4)	Ir-C(2)-O(2)	177 (1)
P(3)-Ir-C(1)	88.2 (3)	C(3)-Os-C(5)	151.2 (4)	Os-C(3)-O(3)	177.9 (8)
P(3)-Ir-C(2)	91.2 (3)	C(4)-Os-C(5)	102.7 (4)	Os-C(4)-O(4)	179 (1)
C(1)-Ir-C(2)	134.3 (4)	Ir-P(1)-C(6)	110.5 (3)	Os-C(5)-O(5)	171.0 (8)
Ir-Os-P(2)	90.57 (5)	Ir-P(1)-C(11)	112.7 (3)		
Ir-Os-P(4)	90.21 (5)	Ir-P(1)-C(21)	119.2 (3)	Torsional Angles	
Ir-Os-C(3)	82.2 (2)	Os-P(2)-C(6)	111.3 (3)	C(1)-Ir-Os-C(3)	-1.8 (5)
Ir-Os-C(4)	171.6 (3)	Os-P(2)-C(31)	115.3 (3)	C(2)-Ir-Os-C(5)	-0.8 (6)
Ir-Os-C(5)	69.0 (3)	Os-P(2)-C(41)	117.8 (3)	P(1)-Ir-Os-P(2)	-1.83 (9)
P(2)-Os-P(4)	174.26 (7)	Ir-P(3)-C(7)	112.1 (3)	P(3)-Ir-Os-P(4)	-1.3 (1)

[a] Numbers in parentheses are estimated standard deviations in the least significant digits.

= Cr, W, $x = 1$, $y = 3$), which involves replacement of the chloride anion in $[RhCl(dppm)_2]$ by the appropriate metal carbonylate anion.[4] This metathesis reaction is accompanied by the transfer of one carbonyl to Rh, the loss of one carbonyl group, and unwinding of the dppm groups to adopt the bridging arrangement. The analogous reaction of a carbonylate anion with $[IrCl(dppm)_2]$ seemed an obvious route into the related heterobinuclear complexes of Ir. However, as will be described, the heterobinuclear complexes obtained display some rather significant differences from the Rh analogues.

Reaction of (PPN)$[HOs(CO)_4]$ with $[IrCl(\eta^2\text{-dppm})_2]$ in THF does not yield the exact analogue of $[RhOsH(CO)_3(dppm)_2]$,[4] diagramed below, although the product, $[IrOs(H)_2(CO)_3(\mu_2\text{-}\eta^3\text{-}(o\text{-}C_6H_4)PhPCH_2PPh_2)(dppm)]$ (1),

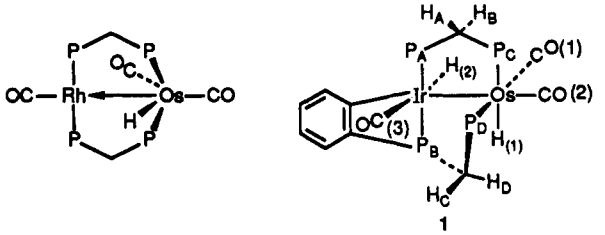

1

is derived from the expected species by ortho metalation of one of the dppm phenyl groups (vide infra). The structure proposed for 1 is based primarily on multinuclear NMR data, although the IR spectrum, the elemental analyses, and the subsequent chemistry are also consistent with the proposal. The carbonyl region of the IR spectrum of 1, displaying a strong band at 1974 cm^{-1} and an envelope at 1915 cm^{-1}, composed of three sharp, closely spaced peaks, establishes that all carbonyls are terminal but otherwise is not very useful for structure elucidation. A weak band is also observed at 2018 cm^{-1} and may be due to a metal–hydride stretch, although this has not been confirmed by deuteration studies. The most significant feature of the IR spectrum, however, is the sharp band at 727 cm^{-1}, which has been attributed to an out-of-plane C–H deformation and appears to be characteristic of ortho-metalated species.[19,20] The most obvious indication that compound 1 is structurally very different from the rhodium analogue is seen in the $^{31}P\{^1H\}$ NMR spectrum, shown in Figure 1A. This spectrum is clearly much different than the two-resonance pattern expected for the AA′BB′ spin system of a simple dppm-bridged species and is instead that of a slightly second-order-distorted ABCD spin system, in which the four chemically unique phosphorus atoms are as labeled in the diagram. All four phosphorus signals fall within the region previously observed for bridging dppm groups.[1-7,21] Our experience with most other dppm-bridged complexes of Ir and Os suggests that the Ir-bound phosphorus nuclei usually resonate downfield from those on Os (see Table I); therefore, the resonance at δ −6.49 is assigned as due to P_A. Assignment of the other resonances is aided by the simulation of this spectrum, shown in Figure 1B, for which the derived parameters are given in Table I. The resonance at δ −17.08 is assigned as P_B on the basis of its large trans coupling (390 Hz) with P_A. Its appearance at ca. 11 ppm upfield from P_A is consistent with it being part of the four-membered, ortho-metalated ring.[22] This leaves the resonances at δ −20.32 and −22.91 as those of P_C and P_D, which are

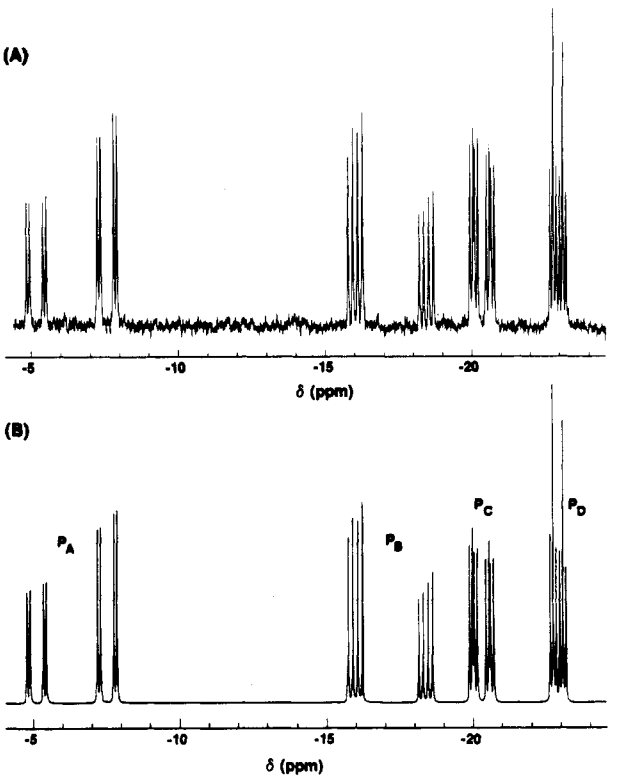

Figure 1. $^{31}P\{^1H\}$ NMR spectra for $[IrOs(CO)_3(H)_2(\mu_2\text{-}\eta^3\text{-}(o\text{-}C_6H_4)PhPCH_2PPh_2)(dppm)]$ (1): (A) observed (in d^8-THF), (B) calculated.

(19) Valentine, J. S. *J. Chem. Soc., Chem. Commun.* **1973**, 857.
(20) Hata, G.; Kondo, H.; Miyake, A. *J. Am. Chem. Soc.* **1968**, *90*, 2278.
(21) Iggo, J. A.; Markham, D. P.; Shaw, B. L.; Thornton-Pett, M. *J. Chem. Soc., Chem. Commun.* **1985**, 432.
(22) (a) Garrou, P. E. *Inorg. Chem.* **1975**, *14*, 1435. (b) Balch, A. L.; Röhrscheid, F.; Holm, R. H. *J. Am. Chem. Soc.* **1965**, *87*, 2301.

attached to Os. The small coupling (17 Hz) between P_C and P_D is consistent with the cis arrangement shown. Owing to the relatively small chemical shift difference between all resonances and the absence of a useful spin-active isotope that would unambiguously establish the metal to which each phosphorus is bound, the proposal that ortho metalation has occurred at Ir instead of Os is not unequivocal but is consistent with the chemical-shift trends noted. The possibility that the phosphorus atoms labeled P_A and P_B are bound to Os instead of Ir can be ruled out on the basis of the observed coupling between these phosphorus nuclei. The value of 390 Hz, obtained from the simulation of the ^{31}P NMR spectrum of **1**, is too large for such coupling across Os, for which values of almost half this appear more appropriate. For example, in related RhOs dimers in which ortho metalation and the trans diphosphine arrangement has occurred at Os, the ^{31}P–^{31}P coupling across Ir is only ca. 230 Hz.[23] In any case, the proposed structure is most consistent with the coordinative unsaturation at Os in the precursor to **1**, which is assumed to be structurally similar to the Rh analogue,[7] and also with the well-documented tendency for low-valent, phosphine complexes of Ir to undergo ortho-metalation reactions.[19,24,25]

Further information about the structure of **1** is obtained from the ^1H and $^{13}C\{^1H\}$ NMR spectra. The high-field region of the ^1H NMR spectrum shows two equal-intensity resonances at δ −9.50 and −12.60, and selective ^{31}P-decoupling experiments indicate that the low-field hydride ($H_{(1)}$) is trans to P_C, displaying a large coupling ($^2J_{PH}$ = 65 Hz) to this nucleus and a smaller coupling ($^2J_{PH}$ = 27 Hz) to the cis phosphorus, P_D. This hydride also shows coupling (7 Hz) to P_A and surprisingly shows a 7-Hz coupling to H_D of the dppm methylene groups. The rather substantial coupling between $H_{(1)}$ and H_D, which is ostensibly four-bond coupling, is more probably a through-space coupling, since in the structure diagramed earlier these two hydrogens appear to be in rather close proximity. The high-field ^1H NMR signal is identified as $H_{(2)}$, the hydride on Ir, owing to its coupling to P_A and P_B, although it is also coupled to P_D (see Table I). Consistent with these data, the $^{13}C\{^1H\}$ NMR spectrum shows one carbonyl resonance (CO(1), δ 189.84) with a large coupling to P_D (88 Hz), indicating that these two are mutually trans, and two other carbonyl resonances that display no resolvable coupling. From the ^{13}C NMR spectrum in which only the low-field hydrogens were decoupled, the carbonyl resonance at δ 180.92 is split into a doublet ($^2J_{HC}$ = 27 Hz) by a hydride ligand, identifying this carbonyl (CO(3)) as the one on Ir. The relative large coupling suggests that these groups have a trans arrangement as shown.[26] Although the relative positions of $H_{(2)}$ and this carbonyl could be interchanged, the large coupling between $H_{(2)}$ and P_D suggests that these groups are trans about the Ir–Os bond (note that $H_{(1)}$ is also coupled to P_A, which is trans across the Ir–Os bond, but not to P_B). Attempts to obtain information about which hydride resonance corresponds to that bound to Os, by utilizing the $[DOs(CO)_4]^-$ anion in the preparation, failed owing to scrambling of the deuterium over both hydride positions. Similarly, we have not succeeded in observing Os satellites associated with either the hydride or carbonyl resonances.

Acidification of compound **1** with 1 equiv of $HBF_4{\cdot}OEt_2$ reverses the ortho metalation, yielding **2**, and treatment of **2** with NaH regenerates **1**. Weaker bases, such as secondary and tertiary amines, do not deprotonate **2**. Com-

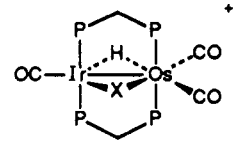

X = H (2)
= AuPPh$_3$ (3)
= I (4)

pound **2** is analogous to the isoelectric species, $[RhOs(CO)_3(\mu\text{-}H)_2(dppm)_2][BF_4]$[7] and $[RhRe(CO)_3(\mu\text{-}H)_2(dppm)_2]$.[6] The $^{31}P\{^1H\}$ NMR spectrum of **2** is characteristic of an AA′BB′ spin system, with resonances at δ 14.11 and 0.52. The high-field signal is assigned to the Os-bound phosphorus nuclei by comparison with the analogous RhOs complex in which the chemical shift for the Os-bound phosphorus nuclei is observed at δ −1.36.[7] The high-field region of the ^1H NMR spectrum of **2** appears as a triplet of triplets δ −9.42, integrating as two hydrogens, and selective ^{31}P decoupling experiments establish that these hydrides couple equally to both sets of phosphorus nuclei ($^2J_{PH}$ = 14 Hz). The symmetric structure shown is also supported by the single resonance observed for the dppm methylene protons, resulting from facile exchange between the axial and equatorial environments, and by the $^{13}C\{^1H\}$ NMR spectrum, which displays one resonance for the two Os-bound carbonyls (δ 180.62) and one for the lone carbonyl on Ir (δ 177.83). The IR spectrum shows three terminal carbonyl bands and a band at ca. 1056 cm^{-1} due to the BF_4^- anion. Attempts to obtain a hydrido methyl complex, analogous to **2**, by reacting **1** with methyl triflate failed since no reaction was observed.

Reaction of **1** with the electrophile, $[AuPPh_3]^+$, yields **3**, assumed to have a structure like that of **2**, based on the comparable spectroscopic data given in Table I and on the isolobality of H^+ and $AuPPh_3^+$.[27] Notable spectroscopic differences between **2** and **3** include the two different dppm methylene resonances observed for **3**, owing to the absence of mirror symmetry about the $IrOsP_4$ plane, and the additional ^{31}P resonance due to the PPh_3 group on Au. Again the chemical shift for the Os-bound phosphorus nuclei is close to that observed in the RhOs analogue.[7]

The reaction of **3** with I_2 yields the iodo-bridged complex, **4**, along with $[Au(PPh_3)I]$ as the other product. The proton and carbon-13 NMR spectra for compounds **3** and **4** are very similar, suggesting that these two compounds have analogous structures. The phosphorus chemical shifts for compounds **3** and **4** differ considerably because the iodo ligand is electronically quite different from the $AuPPh_3$ group, being capable of donating two more electrons when bridging. Analogous differences were noted in the related RhOs compounds,[7] and again the ^{31}P resonances for the Os-bound phosphorus nuclei are closely comparable to those in **4**.

Under a CO atmosphere, compound **2** slowly reductively eliminates H_2 to yield the pentacarbonyl species, **5**, and reaction of this product with H_2 regenerates **2** after about 36 h. The addition of ^{13}CO to compound **5** results in the complete enrichment of all carbonyls in less than 12 h. The spectroscopic data, summarized in Table I, which show two resonances in the $^{31}P\{^1H\}$ NMR spectrum, three terminal carbonyl resonances (δ 199.53, 184.48, 174.13) in a 2:2:1 intensity ratio in the $^{13}C\{^1H\}$ NMR spectrum, no

(23) Hilts, R. W.; Sterenberg, B. T.; Cowie, M. Manuscript in preparation.
(24) Bennett, M. A.; Milner, D. L. *J. Am. Chem. Soc.* **1969**, *91*, 6983.
(25) (a) Bruce, M. I. *Angew. Chem., Int. Ed. Engl.* **1977**, *16*, 73. (b) Clucas, J. A.; Foster, D. F.; Harding, M. M.; Smith, A. K. *J. Chem. Soc., Chem. Commun.* **1984**, 949.
(26) Whitesides, G. M.; Maglio, G. *J. Am. Chem. Soc.* **1969**, *91*, 4980.
(27) Evans, D. G.; Mingos, D. M. P. *J. Organomet. Chem.* **1982**, *232*, 171.

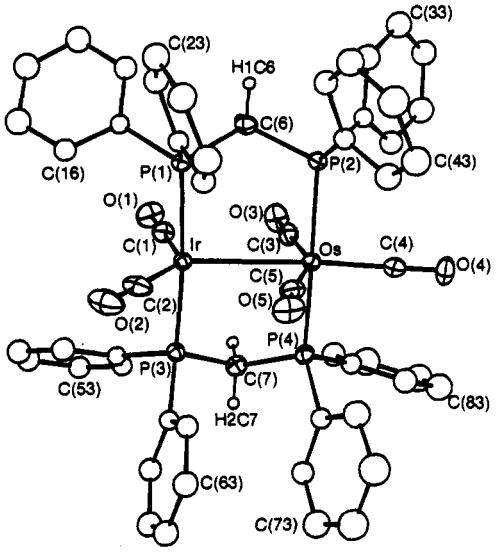

Figure 2. Perspective drawing of the $[IrOs(CO)_5(dppm)_2]^+$ cation showing the numbering scheme. The thermal ellipsoids are shown at the 20% level, except for the methylene hydrogens, which are drawn artificially small.

high-field resonances in the ^1H NMR spectrum, and five carbonyl stretches above 1900 cm^{-1} in the IR spectrum, are consistent with the structure shown. This formulation has been confirmed by an X-ray structure determination (vide infra).

Compound **5** is rather unreactive, in keeping with the coordinative saturation at both metals, and fails to react with activated alkynes (hexafluoro-2-butyne and dimethyl acetylenedicarboxylate) or with trimethylphosphine. Increasing the reaction time and heating the mixtures under reflux in THF succeeded only in producing several unknown decomposition products. The slow reaction with H_2 and ^{13}CO, noted earlier, may result from the lability of the Os → Ir dative bond, creating coordinative unsaturation at Ir, and from the small sizes of the H_2 and CO molecules, which allow access to Ir. Carbonyl loss from **5** can be induced through reaction with $Me_3NO{\cdot}2H_2O$, yielding **6**, proposed to have the structure diagramed. The

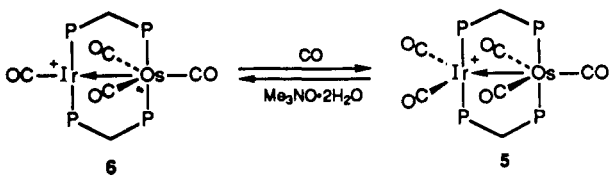

6 **5**

suggestion that carbonyl loss occurs from Ir is consistent with its tendency to adopt a square-planar geometry and 16e configuration and with the large change in ^{31}P chemical shift (ca. 33 ppm) for the Ir-bound phosphorus nuclei upon decarbonylation, while the resonance for the Os-bound phosphorus nuclei remains essentially unchanged. The carbonyl resonances at δ 192.62, 182.30, and 175.30 in a 2:1:1 intensity ratio are also consistent with the structure shown; the two low-field resonances were shown by selective phosphorus decoupling experiments to be due to the three carbonyls on Os. Furthermore, compound **6** is isoelectronic with $[RhOs(CO)_4(dppm)_2]^+$ [7] and $[RhRe(CO)_4(dppm)_2]$ [4] for which the Rh coupling has clearly established that only one carbonyl group is bound to Rh, and the structure determination of the "RhRe" species has clearly established the geometry as shown for **6**. As in previous compounds, the $^{31}P\{^1H\}$ resonance for the Os-bound phosphorus nuclei in **6** is close to that observed (δ–7.27) for the RhOs analogue.[7]

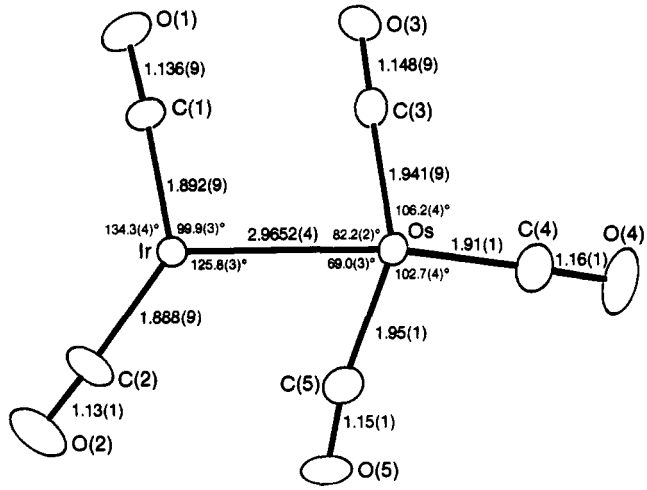

Figure 3. Representation of the metal–carbonyl plane showing some relevant parameters.

Structure of Compound 5. The title compound (**5**) crystallizes with 1.5 equiv of CH_2Cl_2. The geometries of the BF_4^- anion and the solvent molecules are as expected, and there are no unusual contacts involving the solvent and the ions. A perspective view of the cation is shown in Figure 2, and a view of the plane containing the metals and the carbonyl groups, together with some relevant parameters, is shown in Figure 3. More complete compilations of bond lengths and angles are given in Tables IV and V, respectively. As shown in Figure 2, the metals are bridged by the two diphosphines in a trans arrangement at each metal. One metal has two carbonyl groups attached and the other has three. Although crystallographically the two metals are not readily distinguished, the labeling shown in which Os has the three carbonyl ligands attached seems clear based on the loss of one Ir-bound carbonyl to yield **6** (vide supra) and on the analogy of this tetracarbonyl species with the isoelectronic "RhOs" and "RhRe" systems. The solid-state structure is in agreement with the spectroscopic data, apart from the slight asymmetry associated with the carbonyl positions (Figure 3), which apparently results in the crystal from the phenyl group orientations (vide infra). All carbonyls are terminally bound and are close to linear. Although all metal–carbonyl distances are comparable, those involving Ir are somewhat shorter than those on Os. This is opposite to the difference expected based on a comparison of the metal radii[28] but is consistent with the Ir(+I)/Os(0) formulation proposed with the Ir(+I) center expected to have a smaller radius than Os(0). The somewhat longer Os–carbonyl distances may also be a consequence of the greater steric crowding about this metal. The slight bending involving C(5)O(5) (Os–C(5)–O(5) = 171.0 (8)°) is due to the nonbonded contacts involving the ortho-hydrogen atoms; the shortest of these, H(26)–O(5), at 2.40 Å, tends to force O(5) away from Ir, while the H(76)–C(5) contact (2.52 Å) pushes C(5) in the direction of Ir. As a result, the Ir–C(5) separation (2.905 (9) Å) is much shorter than the Ir–C(3) distance (3.316 (8) Å) but does *not* necessarily imply a significant Ir–C(5) interaction.

There are two subtly different ways of considering the bonding in compound **5**. In the first, the positive charge on the complex is localized on Os, yielding Os(+I) and Ir(0) oxidation states and a covalent Os–Ir bond. Alternatively

(28) (a) Wells, A. F. *Structural Inorganic Chemistry*; Clarendon Press: Oxford, 1975; p 1022. (b) Purcell, K. F.; Kotz, J. C. *Inorganic Chemistry*; W. B. Saunders: Philadelphia, PA, 1977; p 528.

the positive charge can be localized on Ir (as diagramed earlier) to give an Ir(+I)/Os(0) formulation. This latter view, in which the metals are in their more conventional oxidation states, would require a donor–acceptor Os → Ir bond. As we have previously discussed,[4,7] the former view would be expected to give a pseudooctahedral coordination at Os, whereas the latter view would give a trigonal bipyramidal (TBP) ligand arrangement (as observed for $[RhM(CO)_4(dppm)_2]$ (M = Mn, Re)), since the dative bond does not appear to require a significant perturbation of the geometry of the *donor* metal.[4,7,8,29] Although for the tetracarbonyl complexes of Mn and Re the geometries at these metals were clearly TBP,[4] the additional carbonyl in **5** results in significant distortions owing to crowding in the complex, so the Os center (ignoring the Os–Ir interaction) is appreciably distorted from the idealized TBP geometry. With consideration of the Os → Ir bond, the geometry at Ir is distorted TBP. The major nonbonded interaction that results in distortions at both the Ir and Os centers involves C(1)–C(11) = 3.18 (1) Å, resulting in opening up of the C(1)–Ir–C(2) angle to 134.3 (4)°. This interaction is substantially shorter than a normal van der Waals contact, which we estimate at ca. 3.6 Å.[30] Movement of C(1) toward Os then causes repulsion of C(3), resulting in a very short C(1)–C(3) contact of 3.03 (1) Å and a concomitant opening of the Ir–Os–C(3) angle to 82.2 (2)° from the 60° expected for an undistorted TBP arrangement. These unfavorable interactions appear to result in a somewhat elongated Os–Ir distance (2.9652 (4) Å), which is slightly longer than typical Os–Os[31] and Ir–Ir[1-3] single bonds, although this separation is still shorter than the intra-ligand P–P distances of ca. 3.06 Å, indicating attraction of the metals. The slight bend of C(4)–O(4) away from the Ir–Os axis appears to result from short contacts involving H(36) (see Table IV).

Conclusions

We have earlier suggested that the compound $[RhOsH(CO)_3(dppm)_2]$ is most appropriately viewed as containing an Os → Rh dative bond connecting the Rh(+I) and Os(0) centers. This view is equivalent to considering the $OsH(CO)_2P_2$ moiety (P = one end of a dppm group) as functioning as a pseudoanion in a square-planar Rh(+I) complex. Such a view has been considered previously for $(OC)Rh(PEt_3)_2Co(CO)_4$[9a,b] and for a series of related dppm-bridged complexes studied within this group.[4-8] One of our interests in studying IrOs analogues of the above RhOs compound was to determine what effect the $OsH(CO)_2P_2$ moiety would have on the oxidative-addition chemistry at the Ir center. The results are dramatically illustrated by our attempt to synthesize $[IrOsH(CO)_3(dppm)_2]$, which instead yields compound **1** through facile ortho metalation of one of the dppm phenyl groups. Not only is this a rare example of ortho metalation involving a dppm group, but it is also the first, of which we are aware, in which ortho metalation has taken place at the same metal to which the phosphorus is bound, forming a highly strained Ir–P–C–C four-membered ring. In addition, this ortho metalation of a Vaska's-type complex is exceptionally facile since invariably such processes require elevated temperatures; it is significant that an ortho-metalated isomer of $[IrCl(CO)(PPh_3)_2]$, formed indirectly from the N_2 complex, $[IrCl(N_2)(PPh_2)_2]$, spontaneously reverts to the more stable non-ortho-metalated species.[19] The facile ortho metalation in the present case suggests that the $OsH(CO)_2P_2$ moiety serves an important function in activating the Ir center toward oxidative addition. The facile reversibility of the ortho-metalation reaction upon protonation and deprotonation also appears to be quite unusual and suggests the potential of novel reactivity upon deprotonation of $[IrOs(CO)_3(\mu\text{-}H)_2(dppm)_2][BF_4]$ in the presence of small molecules, provided that the ortho-metalation reaction can be inhibited.

The structural determination of **5** offers confirmation of previous proposals regarding the natures of labile intermediates involved in ligand substitution reactions involving $[RhOs(CO)_4(dppm)_2]^+$[7] and $[RhRe(CO)_4(dppm)_2]$;[6] it had been assumed that such reactions proceeded by prior coordination of the incoming ligand at Rh to give a structure analogous to **5**. In particular, compound **5** models the labile carbonyl adducts of the above RhOs and RhRe tetracarbonyl species. The synthesis of $[IrOs(CO)_4(dppm)_2][BF_4]$ via CO loss from **5** allows us to investigate chemistry related to that under study in the analogues RhOs and RhRe systems[5-7] with aims of gaining further information about the functions of the adjacent metals in the activation of small molecules.

Acknowledgment. We thank the Natural Sciences and Engineering Research Council of Canada (NSERC) and the University of Alberta for support of this work and NSERC for partial support of the diffractometer. We also thank Professor J. Takats for a loan of ^{13}C-enriched $Os_3(CO)_{12}$ and Professor R. J. Puddephatt for a copy of ref 10a prior to publication.

Registry No. **1**, 132959-03-6; **2**, 132939-86-7; **3**, 132939-88-9; **4**, 132959-05-8; **5**, 132959-02-5; **6**, 132939-90-3; $[IrCl(\eta^2\text{-}dppm)_2]$, 132939-91-4; $[Ir(C_8H_{14})_2(\mu\text{-}Cl)]_2$, 12246-51-4; (PPN)$[HOs(CO)_4]$, 79408-53-0; $[Au(PPh_3)Cl]$, 14243-64-2; Ir, 7439-88-5; Os, 7440-04-2; Au, 7440-57-5.

Supplementary Material Available: Crystallographic data and details of intensity collection and a complete listing of all atom positional and isotropic thermal parameters and complete bond lengths and angles (13 pages); listings of the observed and calculated structure factors (28 pages). Ordering information is given on any current masthead page.

(29) (a) Arndt, L. W.; Darensbourg, M. Y.; Delord, T. I.; Bancroft, B. T. *J. Am. Chem. Soc.* **1986**, *108*, 2617. (b) Woodcock, C.; Eisenberg, R. *Inorg. Chem.* **1985**, *24*, 1285. (c) Breen, M. J.; Shulman, P. M.; Geoffroy, G. L.; Rheingold, A. L.; Fultz, W. C. *Organometallics* **1984**, *3*, 782. (d) Iggo, J. A.; Markaham, D. P.; Shaw, B. L.; Thornton-Pett, M. *J. Chem. Soc., Chem. Commun.* **1985**, 432. (e) Breen, M. J.; Duttera, M. R.; Geoffroy, G. L.; Novotrak, G. C.; Roberts, D. A.; Shulman, P. M.; Steinmetz, G. R. *Organometallics* **1982**, *1*, 1008. (f) Jacobsen, G. B.; Shaw, B. L.; Thornton-Pett, M. *J. Chem. Soc., Chem. Commun.* **1986**, 13. (g) Targos, T. S.; Rosen, R. P.; Whittle, R. P.; Geoffroy, G. L. *Inorg. Chem.* **1985**, *24*, 1375.

(30) We assume that a "normal" van der Waals separation between carbonyls is not much different than that between two aromatic rings, which are in a face-to-face arrangement, owing to a similar interaction between the π-electron clouds.

(31) Churchill, M. R.; DeBoer, B. G. *Inorg. Chem.* **1977**, *16*, 878.